

Mitotic spindle orientation distinguishes stem cell and terminal modes of neuron production in the early spinal cord

Arwen C. Wilcock^{1,2}, Jason R. Swedlow^{2,*} and Kate G. Storey^{1,*}

Despite great insight into the molecular mechanisms that specify neuronal cell type in the spinal cord, cell behaviour underlying neuron production in this tissue is largely unknown. In other neuroepithelia, divisions with a perpendicular cleavage plane at the apical surface generate symmetrical cell fates, whereas a parallel cleavage plane generates asymmetric daughters, a neuron and a progenitor in a stem cell mode, and has been linked to the acquisition of neuron-generating ability. Using a novel long-term imaging assay, we have monitored single cells in chick spinal cord as they transit mitosis and daughter cells become neurons or divide again. We reveal new morphologies accompanying neuron birth and show that neurons are generated concurrently by asymmetric and terminal symmetric divisions. Strikingly, divisions that generate two progenitors or a progenitor and a neuron both exhibit a wide range of cleavage plane orientations and only divisions that produce two neurons have an exclusively perpendicular orientation. Neuron-generating progenitors are also distinguished by lengthening cell cycle times, a finding supported by cell cycle acceleration on exposure to fibroblast growth factor (FGF), an inhibitor of neuronal differentiation. This study provides a novel, dynamic view of spinal cord neurogenesis and supports a model in which cleavage plane orientation/mitotic spindle position does not assign neuron-generating ability, but functions subsequent to this step to distinguish stem cell and terminal modes of neuron production.

KEY WORDS: FGF, Asymmetry, Live imaging, Mitotic spindle, Neurogenesis, Spinal cord, Chick, Stem cells

INTRODUCTION

Spinal cord cells include motor neurons, sensory neurons and multiple classes of interneuron that together mediate movement and sensation of the body. The molecular mechanisms that specify these different kinds of neuron in the spinal cord have been well-characterized (Jessell, 2000; Price and Briscoe, 2004). There is also evidence for crosstalk between patterning factors that regulate cell type and genes that drive cell cycle exit and neuronal differentiation (Scardigli et al., 2003; Scardigli et al., 2001) (reviewed by Bertrand et al., 2002). Neuron production is itself regulated through the Notch signalling pathway; differentiating neurons deliver lateral inhibitory signals, such as Delta1, which ensure that neighbouring cells do not differentiate simultaneously (reviewed by Lewis, 1996). However, despite this wealth of understanding at the level of gene regulation, the cell behaviour underlying neuron production in the spinal cord remains poorly characterized.

The spinal cord is so well-studied because it is a relatively simple neuroepithelium. At early stages it comprises a bilaterally symmetrical tube each side of which is just one cell wide, with each cell contacting both the outer basal and inner apical (ventricular/luminal) surfaces. Within this tissue nuclei migrate between these surfaces and their position reflects progression through the cell cycle; mitosis occurs apically and nuclei move towards the basal surface during G1. After the nuclei arrive at the basal surface, cells then either re-enter S phase or exit the cell cycle

and become neurons. This process, known as interkinetic nuclear migration (Frade, 2002), and subsequent neurogenesis have not been monitored in the spinal cord *in vivo*.

Neurons can be produced by asymmetric, stem cell mode divisions that produce a neuron and a progenitor or by symmetric terminal divisions that produce two neurons. Retroviral labelling studies indicate that both asymmetric and symmetric modes of neuron production underlie sensory neuron generation in the late-stage spinal cord (Wildner et al., 2006). However, the first neurons to be born in the chick spinal cord are reticular spinal interneurons located in dorsal and intermediate regions, followed by ventral motor neurons (Sechrist and Bronner Fraser, 1991), and the modes of division that produce these crucial components of the spinal cord have not been determined.

Work in the mammalian cortex suggests that whether a division generates asymmetric or symmetric cell fates depends on the orientation of the mitotic spindle and hence cleavage plane position with respect to the apical surface of the neuroepithelium (Chenn and McConnell, 1995). A parallel cleavage plane places one daughter cell at the apical surface and the other more basally, whereas a perpendicular cleavage plane generates daughter cells that inherit equal portions of apical and basal membrane; mitotic spindle orientation may thus mediate cell-fate choice, as a parallel cleavage plane could lead to asymmetric segregation of determinants localized at apical or basal surfaces (reviewed by Gotz and Huttner, 2005). Chenn and McConnell propose that in the early cortex perpendicular cleavage plane divisions give rise to two progenitors, whereas parallel divisions generate a neuron and a progenitor (Chenn and McConnell, 1995). This and other studies (Kosodo et al., 2004) thus suggest a link between division orientation and acquisition of a neurogenic (neuron generating) ability.

Experimental evidence for the importance of mitotic spindle orientation for cell-fate choice in the mammalian cortex and retina has come from recent work in which its position has been

Divisions of ¹Cell and Developmental Biology and ²Gene Regulation and Expression, Wellcome Trust Biocentre, College of Life Sciences, University of Dundee, Dow Street, Dundee DD1 5EH, UK.

* Authors for correspondence (e-mail: jason@lifesci.dundee.ac.uk; k.g.storey@dundee.ac.uk)

manipulated by interfering with components of an apical protein complex, including Inscuteable and AGS3 (Betschinger and Knoblich, 2004; Sanada and Tsai, 2005; Zigman et al., 2005). Disruption of this apical complex leads to an increase in perpendicular cleavage plane divisions and in symmetric cell fates. The relationship between cleavage plane orientation and cell-fate choice has not been addressed in the spinal cord, nor is it known whether this tissue, like the cortex, displays a transition from asymmetric to symmetric modes of neuron production as development proceeds. Neuron-generating divisions in the cortex are further distinguished by longer cell cycle times, because of extension of G1 phase (Calegari and Huttner, 2003; Takahashi et al., 1995) (reviewed by Gotz and Huttner, 2005). It has been suggested that a longer G1 allows time for the asymmetric localization and accumulation of cell fate determinants. Although overall cell cycle time gets longer as development proceeds in many neuroepithelia, including the spinal cord (Kauffman, 1968), it has yet to be established whether this is a specific characteristic of all neuron-generating divisions.

Here we have developed a novel long-term time-lapse imaging assay to monitor single cells in the early chick spinal cord as they transit mitosis and then either divide again or undergo neuronal differentiation. Our study defines key parameters of cell behaviour in this tissue and surprisingly reveals that neurons are generated concurrently by symmetric and asymmetric division. Furthermore, we find that mitotic spindle orientation does not correlate with acquisition of neurogenic ability, but serves within neurogenic cells to distinguish modes of neuron production.

MATERIALS AND METHODS

Embryo slice preparation and culture

Embryos at Hamburger and Hamilton (HH) (Hamburger and Hamilton, 1951) stage 9–10 were electroporated using standard techniques (Itasaki et al., 1999), with a concentration of 0.125 $\mu\text{g}/\mu\text{l}$ enhanced yellow fluorescent protein (eYFP)- α -tubulin (BD Sciences/Clontech) and/or Gap43-mRFP1 (Poggi et al., 2005). Embryos were incubated at 38°C for 4 or 16 hours (giving slices for imaging at HH10 and 12). Slices of $\sim 150 \mu\text{m}$ were taken with a microknife, embedded in rat tail collagen type I in coverslip-based petri dishes (WillCo-dish glass-bottom dish, Intracel, Royston, UK; GWst-3522, coated with poly-L-lysine, Sigma) and cultured in Neurobasal medium, without phenol red (Gibco), supplemented with B-27 to a final $1 \times$ concentration with L-glutamine and gentomycin [after Placzek and Dale (Placzek and Dale, 1999)] maintained at 37°C with 5% CO_2/air for ~ 4 hours before imaging. For fibroblast growth factor (FGF) treatment, media containing 200 ng/ml Human FGF4 (R&D Systems) replaced normal medium at the start of the experiment and was changed once (at 18 hours) approximately halfway through the imaging period.

Slice imaging

Slices were imaged on a DeltaVision Spectris microscope workstation (Applied Precision, LLC, Issaquah, WA) in a Solent environmental chamber kept at 37°C. The chamber stage was buffered with 5% $\text{CO}_2/95\%$ air mix and maintained in a humid environment. Images were captured using a 40×1.35 NA objective lens with the Hg-arc lamp. Thirty optical sections (exposure time=50 milliseconds, 512×512 pixels, bin=2) spaced by $1 \mu\text{m}$ to $2.5 \mu\text{m}$ were imaged at either 7-minute or 1.5-minute intervals, for up to 38 hours. The point-visiting function in the software allowed up to eight slices to be imaged during each experiment. Data was deconvolved and analyzed using constrained iterative deconvolution (McNally et al., 1999; Swedlow, 1997). At the end of time-lapse experiments, slice culture dishes were immediately washed in 37°C PBS and fixed in fresh 37°C 4% formaldehyde (FA) for 40 minutes to preserve microtubules/eYFP- α -tubulin, washed in PBS and 37°C PBS 0.5% Triton X-100, and subsequently labelled with antibodies against GFP and neuronal markers (see below).

Analysis of neuron production

Embryos at day 1.5 (HH10), day 2 (HH13), day 2.5 (HH16) and day 3 (HH18–19) were fixed in fresh 4% FA and subjected to in situ hybridization for *NeuroM* (Roztocil et al., 1997), a bHLH transcription factor that marks newly born neurons (Diez del Corral et al., 2002; Roztocil et al., 1997) (see below), using standard techniques. Sections through neural tube were then processed for immunocytochemistry for HuC, an RNA binding protein characteristic of differentiating neurons (Marusich et al., 1994) (see below), followed by staining with the chromatin marker DAPI.

Measurement of cell cycle and mitosis duration

Embryos at HH10 were exposed to 100 μl of 0.1 mM BrdU for 1 hour or 4 hours, fixed in 4% FA and processed and cryosectioned using standard techniques (three embryos per treatment, four sections from each embryo). Sections were treated using standard immunocytochemistry techniques, post-fixed in 4% FA for 10 minutes and subjected to a standard BrdU detection protocol (Gunhaga et al., 2000). Total progenitor cell population was determined by subtracting calculated proportion of differentiated neurons (3%, see Fig. S1 in the supplementary material) from total cell number, and simultaneous equations were used to calculate cell cycle time (Storey, 1989). Mitotic cells were determined by distinct morphology of DAPI-stained nuclei undergoing mitosis at the apical surface, and M-phase duration was calculated using cell cycle time and mitotic index (see Fig. S2 in the supplementary material).

Cell death assessment

Embryos at 1.5 and 3 days were fixed in FA, processed and cryosectioned using standard techniques. Sections through neural tube flanked by somites 1–3 were then processed for immunocytochemistry for cleaved Caspase-3 (see below) and stained with DAPI. Apoptotic cells were scored in four sections in three embryos for each timepoint, day 1.5 ($1 \pm 0.6\%$) and day 3 ($0.2 \pm 0.05\%$) (s.d. is the variance between embryos). Images of cells in slice culture were analyzed for apoptosis (characteristic blebbing and eruption of cells) at 16 hours in time-lapse movies (15 slices, four experiments) ($1.5 \pm 0.5\%$) (s.d. is the variance between experiments). The number of cells undergoing apoptosis and the total number of labelled cells visible at this time were recorded. This was used to calculate the proportion of cells dying at a fixed timepoint, which could then be compared with that observed in fixed tissue sections.

Measurement of cleavage plane orientation

Embryos at day 1.5 and 3 were fixed in fresh 4% FA and stained with DAPI. The angle of the cleavage plane of cells in anaphase and telophase was measured relative to the apical surface of the neural tube in sections through neural tube flanked by somites 1–3 (in 10–12 sections from three to four separate embryos). Images were captured on a Leica DM IRB, 20×0.3 NA lens with a Hamamatsu Snapper DIG16 camera. Data were analyzed onscreen using OpenLab (Improvision) software. In slice cultures the apical surface was identified by the position of the flattened end feet of cell processes, which form the lumen wall. When the lumen is not absolutely vertical, stereoscopic viewing of the images was used to determine the position of a dividing cell in relation to the apical surface. Visualization of the lumen was also assisted by brightfield images. To measure the angle of the cleavage plane relative to the apical surface, data was rendered into a three-dimensional view (using the volume viewing tool in Softwrx software) and assigning the lumen (apical surface) to the horizontal plane. The image was then rotated around 360° in the y-axis to enable accurate measurement of the angle bisecting the two daughter cells at cytokinesis [similar to the rendering and angle measurements made in Haydar et al. (Haydar et al., 2003)].

In situ hybridization and immunocytochemistry

Standard whole-mount in situ hybridization techniques were performed to detect *NeuroM*. Immunocytochemistry was also performed using standard procedures. Differentiated neurons were detected using mouse anti-HuC/HuD (1:200) (Molecular Probes, A-21271) or mouse anti-neurofilament-associated antigen 3A10 (1:50) (Developmental Studies Hybridoma Bank). Cleaved Caspase-3 (Asp175) rabbit monoclonal antibody (Cell Signalling, 9664) was used to detect apoptotic cells,

following the manufacturer's instructions. YFP signals in slice cultures were enhanced with a rabbit anti-GFP (1:100) (MBL, 598) after the imaging period. BrdU was detected with sheep anti-BrdU (1:100) (AbCam, ab1893). Secondary antibodies used were anti-mouse Alexa Fluor-488 (1:500) (Molecular Probes, A21121), anti-mouse Alexa Fluor-568 (1:200) (Molecular Probes, A-11031), or anti-mouse Rhodamine Red (1:200) (Jackson ImmunoResearch, 715-295-150), anti-sheep FITC (1:200) (Jackson ImmunoResearch, 713-095-147), anti-rabbit biotin (1:1000) (Jackson ImmunoResearch, 111-065-144) with Cy3-conjugated streptavidin (1:4000) (Jackson ImmunoResearch, 016-160-084), and anti-rabbit Alexa Fluor-488 (1:200) (Molecular Probes, A-21206).

Statistical analysis

Statistics were performed using either Minitab or Sigma Stats. Statistical tests are justified in the Figure legends. In all descriptive statistics where sample means are used, variance is indicated by 1 s.d.

RESULTS

Imaging neurogenesis in embryo slice culture

To elucidate cell behaviour underlying neurogenesis in the early spinal cord we used low-level electroporation to introduce a plasmid driving expression of eYFP- α -tubulin and/or GAP43-mRFP1 into the neural tube of day 1.5 chick embryos (stage HH10). Whole embryo slices were taken between the level of somites 1-6 and each slice embedded in collagen on a coverslip-based petri dish and maintained in serum-free medium (Fig. 1A). Using a low concentration of plasmid we labelled ~5% of the cells located in dorsal and intermediate regions of the neural tube, allowing easy visualization of the microtubule cytoskeleton (eYFP- α -tubulin) and cell membrane (GAP43-mRFP1) of individual cells. Time-lapse, three-dimensional fluorescence images were recorded on a wide-field DeltaVision imaging system and subjected to image deconvolution (McNally et al., 1999; Swedlow, 1997). In all cases, we recorded three-dimensional data stacks spanning at least 30 μ m at 7-minute intervals for up to 38 hours, unless otherwise stated (see Materials and methods). This imaging period corresponds to development from HH10/11 to ~HH16, during which newly born neurons rise from 3 to 15% of cells in the neural tube (see Fig. S1 in the supplementary material).

To validate this approach we compared cell cycle time, length of mitosis and incidence of cell death in this region of the neural tube at day 1.5 in fixed embryos with that observed in neural tube in slices subjected to our imaging protocol. In fixed tissue, the proportion of cells incorporating BrdU at two separate timepoints indicated a cell cycle time of ~16 hours (see Materials and methods and Fig. S2 in the supplementary material). In living slices, cell cycle times were directly determined from the length of time between cell divisions. These show striking heterogeneity, ranging from ~9 to 28 hours (87 cells in 20 slices; see Fig. S2 in the supplementary material) but with an average (16 hours 10 minutes \pm 4 hours) similar to that calculated in our fixed tissue and in the zebrafish hindbrain (Lyons et al., 2003). The duration of mitosis in slices (28 \pm 9 minutes) was similar to that calculated in the embryo (32 \pm 8 minutes), indicating that imaged cells are not delayed at cell cycle checkpoints (see Materials and methods and Fig. S2 in the supplementary material). Immunocytochemical detection of the cleaved form of Caspase-3, characteristic of apoptotic cells, also indicated that imaging does not increase the incidence of cell death: similar proportions of apoptotic cells were observed in sections of fixed neural tube at day 1.5 (1 \pm 0.6%) and day 3 (0.2 \pm 0.05%) and in imaged slices at 16 hours (1.5 \pm 0.5%) (see Materials and methods). These findings indicate that cell behaviour in these tissue slices is comparable to that observed in the embryo and that this tissue slice assay can be used for detailed analysis of normal cell behaviour in the chick neural tube.

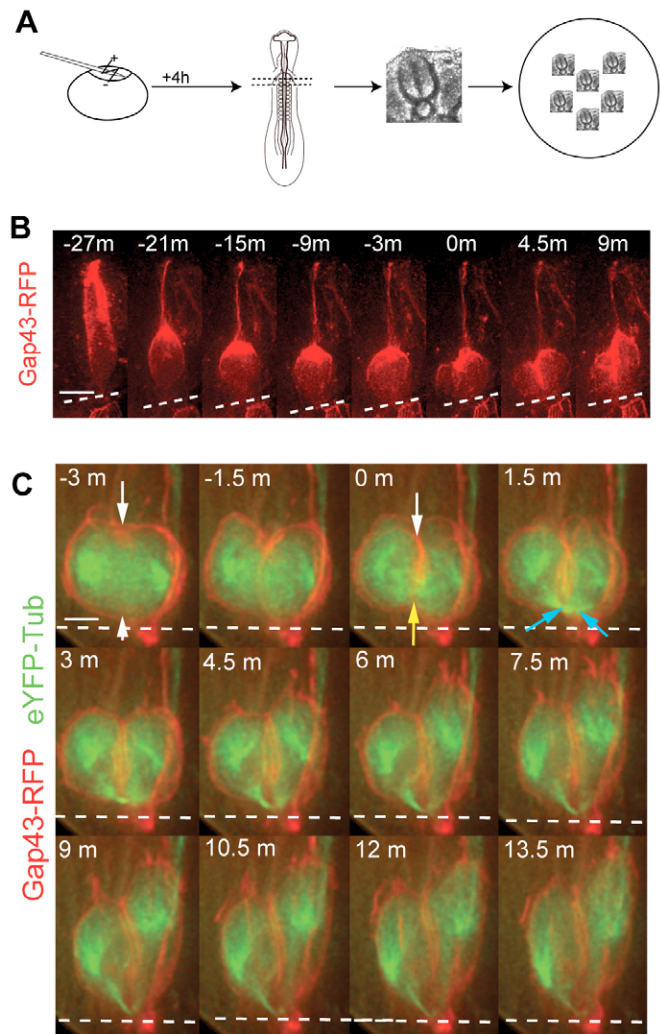


Fig. 1. Cell behaviour during mitosis in the early neural tube.

(A) Slice culture method; DNA is electroporated into the neural tube, embryo slices mounted on coverslip-based dishes and imaged on a Deltavision widefield microscope. (B) Cell membrane label (Gap43-mRFP1) reveals basal process retention during mitosis. Maximum intensity projections (MIP) of 15 z-sections, captured at 2.5 μ m intervals. White broken line indicates the apical surface; scale bar: 10 μ m. (C) Gap43-mRFP1 (red) visualizes initiation and progression of the cleavage furrow around the centre of the dividing cell (white arrows), whereas eYFP- α -tubulin (green) reveals the mitotic spindle, formation of the midbody by the central mitotic spindle (yellow arrow) and the contribution of this structure to two new apical processes on completion of cytokinesis (blue arrows). Images are MIP of 15 z-sections of each wavelength captured at 2.5 μ m at 1.5-minute intervals. (See Movie 1 in the supplementary material.) Scale bar in C, 10 μ m.

Cell behaviour during interkinetic nuclear migration and neuron birth

To monitor cellular dynamics during neurogenesis in the spinal cord, cells were labelled with GAP43-mRFP1 alone and/or YFP- α -tubulin. Labelling the cell membrane with GAP43-mRFP1 revealed that as cells round up on division at the apical surface they retain a thin membranous process that is inherited by one daughter cell in all divisions in which we were able to observe this structure ($n=12$ cells) (Fig. 1B). Following initiation of the cleavage furrow revealed

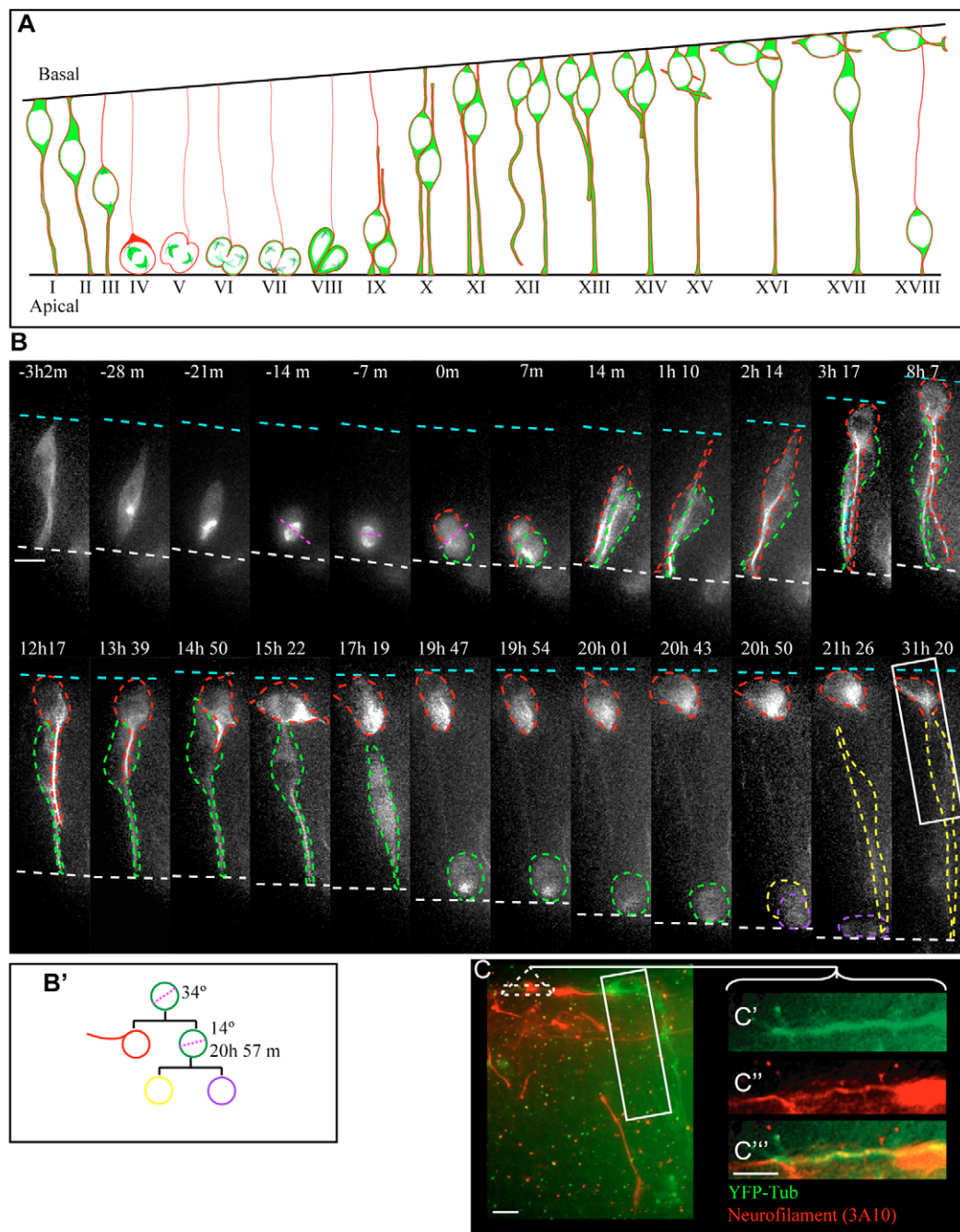


Fig. 2. Neuron birth and asymmetric neuron production. (A) Schematic of neuron birth: green, α -tubulin; red, cell membrane. I-III, migration of nuclei to apical surface \sim 3 hours; IV-VII, mitosis \sim 30 minutes; VIII-XI, apical-basal nuclei migration \sim up to 9 hours post-mitosis; XII-XVI, release and retraction of the apical process, up to 15 hours and 25 hours post-mitosis, respectively; XVI-XVIII, cell body reorientation, production of an axon and return of sibling cell nucleus to apical surface for further division (times for five cells). (B) Asymmetric neuron production: a cell divides to produce a neuron (red dashed outline) and a progenitor cell (green dashed outline). Pink broken line indicates the cleavage plane. White broken line indicates apical surface. Blue broken line indicates basal surface. White box in final frame indicates region for comparison in C. Scale bar: 10 μ m. Each image is a MIP through 30 z-sections imaged at 1.5 μ m intervals. (B') Lineage tree for cells in B. (See Movie 2 in the supplementary material.) (C) Immunocytochemistry to confirm neuronal identity of the cell in B marked by a red dashed outline. Axonal process from eYFP-positive cell (green) in final stills frame (white box in B, and see Movie 2 in the supplementary material) labelled with 3A10 (red, a monoclonal antibody that recognizes a neurofilament-associated protein). MIP through 30 z-sections imaged at 1.5 μ m intervals. Scale bar: 10 μ m. (C'-C''') Region framed by dashed box in C. (C') eYFP; (C'') 3A10 labelling; (C''') eYFP/R merge. MIP through 3 μ m of the field in view; scale bar: 5 μ m.

with GAP43-mRFP1, a midbody identified with eYFP- α -tubulin forms between the two halves of the cell and then becomes displaced towards the apical surface (Fig. 1C, Fig. 2A; see Movie 1 in the

supplementary material). This structure, a remnant of the mitotic central spindle (Glotzer, 2005; Nagele and Lee, 1979) consisting of a dense concentration of microtubules and many microtubule-

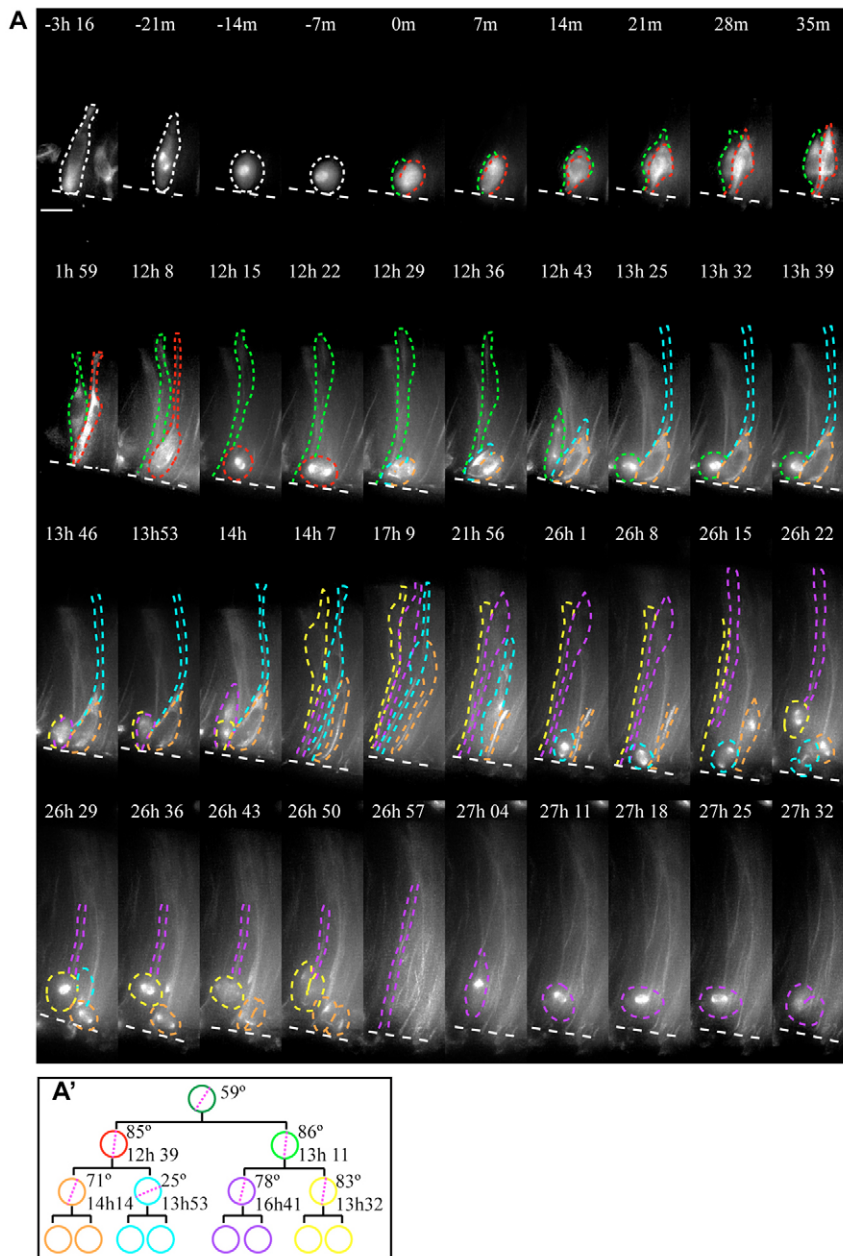


Fig. 3. Progenitor-generating divisions. (A) A progenitor-generating lineage. The nucleus of the mother cell (white dashed outline) migrates apically (white broken line) and divides to produce two daughter progenitors (red and green dashed outlines). These cells divide again, producing four progenitor cells (yellow, orange, blue and purple dashed outlines) that each divide once more. MIP through 30 z-sections imaged at 1.5 μm intervals; scale bar: 10 μm . **(A')** Lineage tree for A. (See Movie 3 in the supplementary material.)

associated proteins (Skop et al., 2004), relocated in all 25 cases examined to form the new apical process in each daughter cell (Fig. 1C, Fig. 2A; see Movie 1 in the supplementary material). The resumption of interkinetic movement following division is then accompanied by the movement of eYFP- α -tubulin into the basal process (Fig. 2B; see Movie 2 in the supplementary material). Once nuclei of both sibling cells have migrated to the basal side of the neuroepithelium, cells may then remain in this configuration in contact with both apical and basal surfaces for up to 15 hours ($n=5$ cells) (Fig. 2A; see Movie 2 in the supplementary material). If a cell is going to differentiate into a neuron, the endfoot of its apical process then releases from the apical surface and the process appears to lose tension. The apical process, as visualized with eYFP- α -tubulin, then gradually withdraws across the surface of neighboring cells until it disappears into the basally located cell body (Fig. 2A,B). A striking reorientation of the polarity of the cell is then manifest, such that it is shifted by 90° and the cell now extends processes

along the dorsoventral, rather than mediolateral, axis of the neural tube (Fig. 2A,B; see Movie 2 in the supplementary material). Subsequent fixation and labelling demonstrated that such cells express neuronal markers (neurofilament or HuC; Fig. 2C) in 19/19 cases (six slices, three separate experiments), confirming that these novel and dramatic changes in cell morphology are indicative of neuron birth.

Two modes of neuron production in the early chick neural tube

To determine the division modes underlying neuron production in the early neural tube we monitored the generation of individual lineages. Each lineage comprises at least one complete cell cycle, i.e. the generation of two daughter cells by mitosis at the apical surface and the subsequent re-entry into mitosis of at least one of these daughter cells and/or neuronal differentiation. Progenitor cells were identified by their completion of a second successful cell

division, whereas cells that became neurons exhibited the striking stereotyped series of morphological changes described above. Of the 51 lineages monitored, 34 involved only progenitor-generating divisions (referred to hereafter as PP divisions) (Fig. 3; see Movie 3 in the supplementary material), whereas the remaining 17 lineages produced neurons (Table 1). Of these, seven exhibited an asymmetric mode of division, producing a neuron and a further progenitor (referred to hereafter as PN divisions) (Fig. 2B; see Movie 2 in the supplementary material), and another six gave rise to two neurons each (referred to hereafter as NN divisions) (Fig. 4; see Movie 4 in the supplementary material) (four more lineages produced a neuron and a sibling of undetermined fate). This indicates that asymmetric and symmetric modes of neuron production take place concurrently in the early spinal cord.

A correlation between mitotic spindle orientation and neurogenic cell fate symmetry

To examine the relationship between mitotic spindle/cleavage plane orientation and cell-fate choice we first wished to establish that similar proportions of cells divide in particular orientations with respect to the apical surface in tissues fixed immediately or monitored *in vivo*. Cleavage plane orientations were measured relative to mitotic spindle position in fixed/DAPI-stained sections of the neural tube at day 1.5 and 3 and in living tissue slices spanning this developmental interval (see Materials and methods). Histograms of these measurements after binning the data into 30° ranges (Fig. 5A,B) show that cells dividing with cleavage planes in all orientations were observed. We did not detect a preferential orientation at day 1.5 in fixed samples, whereas by day 3 we observed a slight preference for either parallel (28%) or perpendicular (58%) orientations (Fig. 5A). In living tissue, imaged from day 1.5 to day 3, cleavage planes were still more likely to be perpendicular to the apical surface and least likely to be parallel (Fig. 5B). These live data broadly correspond with the spread of division orientations observed in fixed tissue over this time period and we find no statistically significant difference between these data sets (Fig. 5A,B). We also made measurements of 20 cleavage plane angles in movies with data taken at 1.5-minute intervals of cells double-labelled

Table 1. Cleavage plane orientation and cell fate choice

Division type	Total divisions	0-30° parallel	30-60° intermediate	60-90° perpendicular
PP	34	6	7	21
NN	6	0	0	6
PN	7	1	3	3
?N	4	2	0	2
Totals	51	9	10	32

Divisions in which both cleavage plane orientation and subsequent daughter cell fates were ascertained: PP, divisions that generate two further progenitors; NN, divisions that generate two neurons; PN, divisions that generate a progenitor and a neuron; ?N, divisions that generate a neuron and a daughter of indeterminate fate. A two-tailed Mann-Whitney U-Wilcoxon rank sum test with a 95% confidence interval was used for pairwise comparison of these data. This shows that data distribution about the median value of PP and NN division orientations is different ($P=0.017$), as is that of NN and PN division orientations ($P=0.006$), but does not support a difference between PP and PN division orientations ($P=0.28$).

with eYFP- α -tubulin and the cell membrane marker Gap43-mRFP1 to help visualize the cleavage furrow. These movies allowed us to confirm that our measurement of final cleavage plane position is accurate *in vivo* using data collected at 7-minute intervals (see Fig. 5C; see Movie 1 in the supplementary material).

Having established that the range of cleavage plane orientations observed *in vivo* is representative of normal cell behaviour, we investigated the relationship between cleavage plane orientation and the subsequent fates of daughter cells. This was analyzed in 47 lineages and in all cases we were able to identify all cells at all time points and determine the position of basal and apical surfaces (Table 1). Of the 34 cells undergoing PP divisions, the majority (21/34, 62%) divided with a perpendicular cleavage plane (Fig. 3; see Movie 3 in the supplementary material; Table 1). By contrast, all six cells that divided to give rise to two neurons exhibited a perpendicular cleavage plane (see Table 1) (Fig. 4; see Movie 4 in the supplementary material). We conclude that there is a good correlation between generation of symmetric neuronal fates and a perpendicular cleavage plane and that symmetric progenitor-generating divisions are not exclusively perpendicular, although they show a tendency to divide with this orientation.

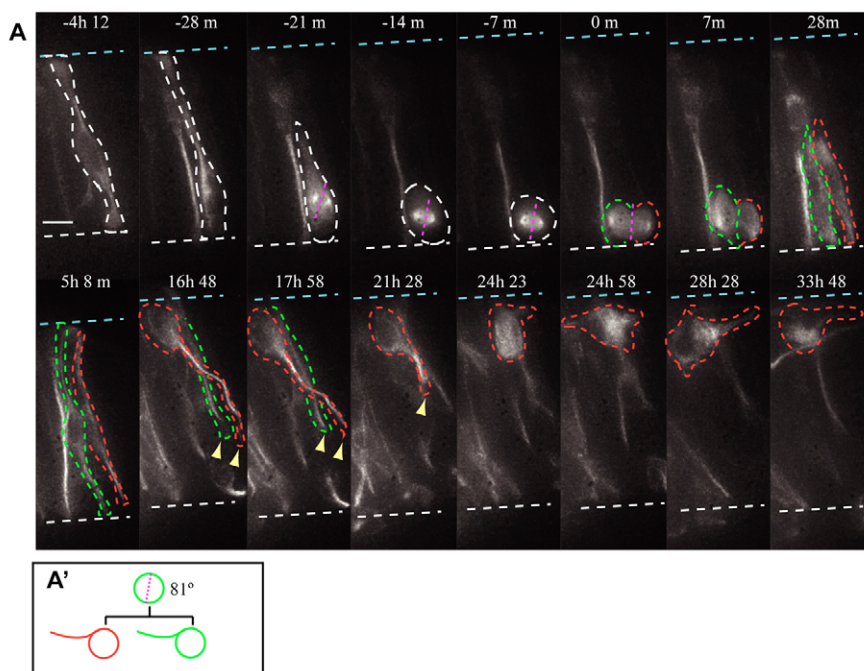


Fig. 4. Symmetric neuron production. (A) A terminal division producing two neurons. The nucleus of a cell (white dashed outline) migrates apically (white broken line) and divides. The cleavage plane (pink broken line) is perpendicular to the apical surface. Following mitosis the two daughter cells (red and green dashed outlines) maintain apical attachment and their nuclei migrate back towards the basal surface (blue broken line). Once the nuclei are at the basal surface both apical processes withdraw. The nucleus of the cell outlined in green becomes obscured, but three-dimensional analysis confirms that it also continues to withdraw its apical process (yellow arrowhead). Scale bar: 10 μ m. Each image is a MIP through 30 z-sections imaged at 1.5 μ m intervals. (A') Lineage tree for A. (See Movie 4 in the supplementary material.)

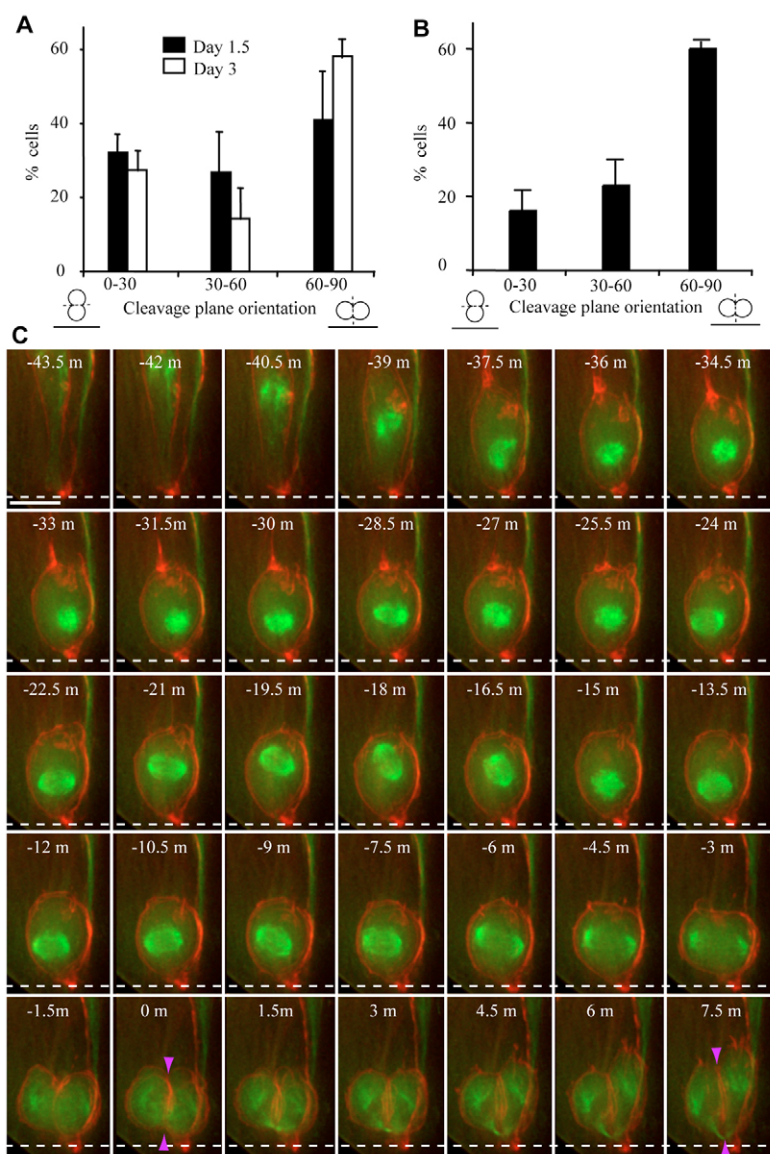


Fig. 5. Cleavage plane orientations in fixed and live tissue.

(A) Orientation of the cleavage plane in anaphase/telophase cells measured in DAPI-stained fixed 1.5- and 3-day-old embryos. Day 1.5 embryos ($n=4$ embryos), 198 divisions; day 3 embryos ($n=3$ embryos), 186 divisions. Error bars represent s.d. (B) Orientation of cleavage plane scored at cytokinesis in tissue slices taken at 1.5 days and cultured for up to 38 hours. Errors bars represent s.d.: 84 divisions, 12 slices, three experiments. An analysis of variance (ANOVA) test comparing cleavage plane orientation of cells in fixed tissue (data from A, pooling 1.5- and 3-day-old embryos) with cells in live tissue (data from B) shows no difference in the distribution of cleavage plane orientations in fixed and live tissue ($P=0.2$). (C) Mitotic spindle movements, cytokinesis and final cleavage plane orientation monitored at 1.5-minute intervals in cells labelled with Gap43-mRFP1 (red) and eYFP-tubulin (green). Cleavage plane orientation is maintained for at least 7.5 minutes post-cytokinesis (purple arrows); mean change in cleavage plane was $3.6 \pm 2.7^\circ$ ($n=20$ cells). Broken line indicates the apical surface; scale bar: $10 \mu\text{m}$. (See Movie 1 in the supplementary material.)

Strikingly, in contrast to the NN divisions the seven PN-generating divisions had cleavage planes in any orientation. For example, Fig. 2B (see Movie 3 in the supplementary material) shows a lineage arising from a division that generated a neuron and a progenitor with a cleavage plane orientated 34° relative to the apical surface, followed by division of the daughter progenitor cell with a cleavage plane at 14° to the apical surface. However, another PN division had a cleavage plane at 75° (Fig. 6; see Movie 5 in the supplementary material). One explanation for this last division comes from observations in the mammalian cortex where only small differences about the perpendicular axis appear sufficient to asymmetrically apportion apical membrane between daughter cells (Kosodo et al., 2004). Indeed, we find that all but one of the NN divisions are oriented greater than 80° and are thus closer to perpendicular than the PN divisions (see dot plot of all cleavage plane orientations, Fig. 6B). Furthermore, statistical comparison of PN and NN division orientations indicates that these are distinct groups (see Table 1).

Importantly, knowing the cell fate outcome of divisions with specific cleavage plane orientations provides further insight into the role of mitotic spindle orientation in cell-fate choice. Our data

indicate that many divisions with a parallel cleavage plane (6/9) give rise not to a neuron and a progenitor, but to two progenitors (Table 1). Simply positioning the mitotic spindle along the apico-basal axis (parallel cleavage plane) is therefore insufficient to generate asymmetric cell fates in this context. Furthermore, statistical comparison provides no evidence for a difference between PN and PP divisions that occur in all orientations, whereas NN division orientations are all perpendicular and are statistically different from PP as well as PN divisions (Table 1). Together, these data suggest that regulation of mitotic spindle position is only crucial within cells that have neuron-generating potential and, moreover, that assignment of this neurogenic ability is separable from division orientation.

Cell cycle length predicts cell fate

Work in the developing mammalian cortex suggests that neuron-generating divisions are characterized by a longer cell cycle than progenitor-generating divisions and that this provides time for daughter cells to become different (Calegari et al., 2005; Calegari and Huttner, 2003; Takahashi et al., 1995). Here we use our direct

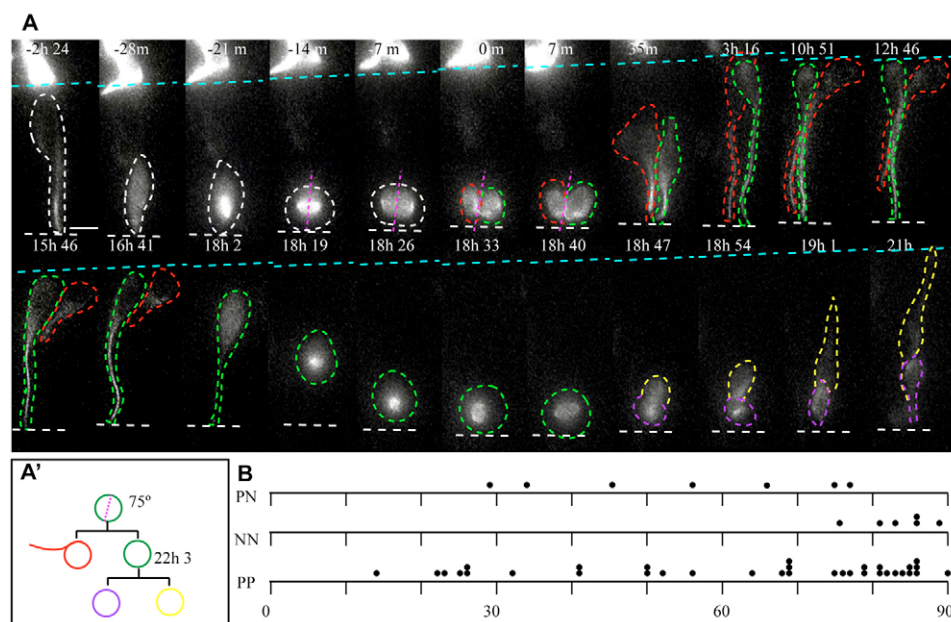


Fig. 6. A perpendicular cleavage plane division giving asymmetric fates. (A) A cell (white dashed outline) divides with a perpendicular cleavage plane (pink broken line) to generate a neuron (red outline) and a progenitor (green outline). Apical processes of both daughter cells are visible as their nuclei migrate back to the basal surface (blue broken line). The nucleus of one cell (red outline) reaches the basal surface first and starts to withdraw its apical process, whereas its sibling (green outline) continues back to the apical surface and divides again; the differentiating daughter cell (red outline) is photobleached in the last frames. Scale bar: 10 μm . Each image is a MIP through 30 z-sections taken at 1.5 μm intervals. (A') Lineage tree for A. (See Movie 5 in the supplementary material.) (B) Dot plot showing cleavage plane orientations of all cells, the progeny of which could be followed to subsequent division or terminal differentiation.

visualization of mitosis and neuron formation to make these measurements for the first time in the spinal cord. We find that in the chick neural tube the cell cycle length of cells dividing to produce one neuron and one progenitor is longer than that for cells that generate only further progenitors (see Fig. 7A). These data support a role for cell cycle extension in the acquisition of the ability to generate neurons.

FGF is known to inhibit neuronal differentiation in many contexts, including chick neural tube explants taken from the same region as our slices (Diez del Corral et al., 2002). Here, FGF has been shown to inhibit expression of a bHLH transcription factor, *NeuroM* (Diez del Corral et al., 2002), which acts within the neurogenesis cascade that leads to neuronal differentiation (Roztocil et al., 1997). We therefore next assessed whether this loss of neuron-generating ability in response to FGF signalling is also accompanied by a decrease in cell cycle length. All 30 lineages analyzed in FGF-treated slices consisted of only progenitor-generating divisions. All of these lacked the apical process release and withdrawal behaviour that is characteristic of newly born neurons (Fig. 7B; see Movie 6 in the supplementary material). Exposure to FGF did not alter the range of cleavage plane orientations of divisions at the apical surface (Fig. 7C). This finding indicates that FGF does not attenuate neuron production by directing mitotic spindle position. Importantly, the cell cycle length of cells in neuroepithelium exposed to FGF was similar to that of normal progenitor-generating PP divisions (Fig. 7A), but shorter than those of PN divisions (Fig. 7A), consistent with all cells behaving as progenitor generators. In a subset of FGF-treated lineages we also observed additional novel cell behaviours, including incomplete interkinetic nuclear migration movements and increased non-apical divisions (Fig. 7D) characterized by even shorter cell-cycle times that are statistically different from PP, PN and apically dividing cells in FGF-treated tissue (see Fig. 7A,B,B'; see Movie 6 in the supplementary material). These data indicate that loss of neurogenic factors in the presence of FGF is accompanied by adoption of a more rapid cell cycle characteristic of cells that only generate further progenitors.

DISCUSSION

Cell behaviour during neurogenesis

Our analysis of cell behaviour within the living spinal cord reveals the presence of a dynamic cell population that exhibits dramatic and sequential changes in cell shape and subcellular organization during progression through the cell cycle and neuronal differentiation. The retention of a thin basal process composed of membrane and lacking microtubules as cells undergo mitosis at the apical surface confirms that cells maintain contact with both basal and apical surfaces throughout the cell cycle (see Afonso and Henrique, 2006). A similar membranous basal process has been observed in other neuroepithelia (Das et al., 2003; Miyata et al., 2001; Saito et al., 2003) and the relocation of eYFP-tubulin into this structure following mitosis is consistent with a microtubule-based mechanism mediating interkinetic nuclear migration movements (Messier and Auclair, 1974). The apical displacement and incorporation of the microtubule-rich midbody into the new apical processes on completion of cytokinesis is the first observation that the post-mitotic midbody gives rise to a specific structure.

Importantly, we demonstrate that all cells in the early spinal cord, whether prospective progenitors or neurons, possess an apical and basal process and exhibit nuclear movement towards the basal surface following mitosis. Prospective neurons with basally located nuclei retain this apical process (see Minaki et al., 2005) and may do so for many hours prior to the first morphological manifestation of neuronal differentiation; the release of this process from the apical surface. This step must thus involve loss of junctional complexes, including adherens junctions (see Afonso and Henrique, 2006), between the differentiating cell and its neighbours. A similar behaviour has also been reported prior to neuronal differentiation in the mammalian cortex, although here prospective neurons do not retain apical contact but migrate away and then form a new process that extends to the apical surface and is retracted on differentiation (Noctor et al., 2004). In the early spinal cord, this loss of apical contacts is followed by reorganization of the microtubule cytoskeleton as the apical process is withdrawn towards the cell body, which then becomes

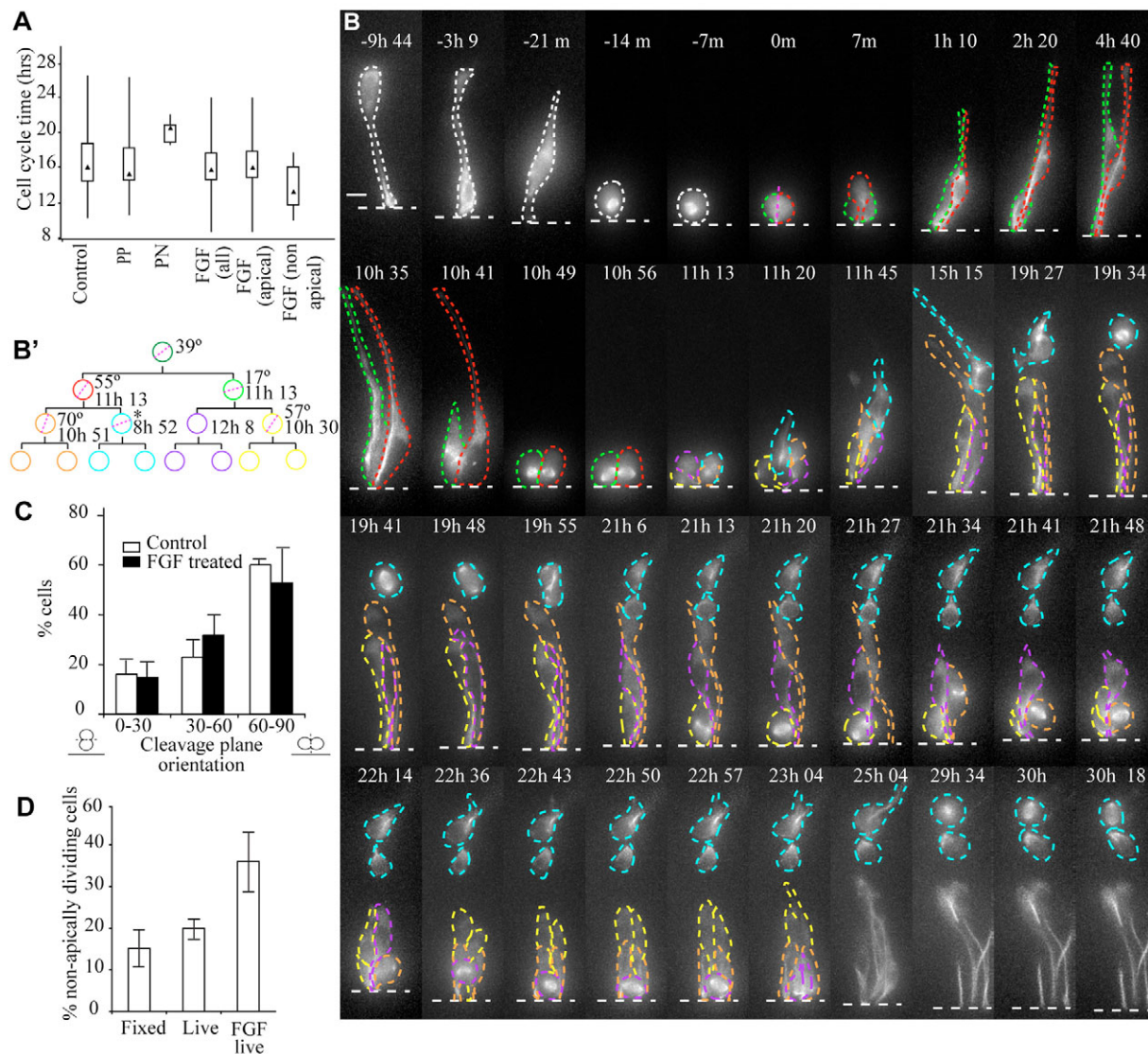


Fig. 7. Neurogenic divisions have a longer cell cycle and FGF accelerates cell cycle. (A) Cell cycle times for divisions in control (untreated) and FGF-exposed slices. Box plot showing quartile ranges for cell cycle times of all control cells (PP+PN divisions, $n=54$); PP divisions ($n=49$); PN divisions ($n=5$); following exposure to FGF, all divisions ($n=65$); apically localized divisions ($n=57$); non-apical divisions ($n=8$). Statistical comparison was performed using the non-parametric two-tailed Mann-Whitney U-Wilcoxon rank sum test for pairwise comparison, as our data sets are not normally distributed; a P -value of <0.05 provides evidence that there is a 95% chance of a difference between compared data. PP compared with PN divisions, $P=0.013$; apical FGF compared with PP divisions, $P=0.632$; apical FGF compared with PN divisions, $P=0.01$; non-apical FGF compared with PP, $P=0.048$; with PN, $P=0.002$; and with apical FGF divisions, $P=0.048$. (B) Exposure to FGF produces only progenitor-generating divisions. A single cell located basally for ~ 10 hours in the presence of FGF divides apically to produce two daughter cells (red and green dashed outlines), which exhibit attenuated interkinetic nuclear migration. Some nuclei also divide non-apically (blue dashed outline). MIP of 30 images captured at $1.5 \mu\text{m}$ intervals. Scale bar: $10 \mu\text{m}$. (B') Lineage tree for cells represented in B. (See Movie 6 in the supplementary material.) (C) Comparison of cleavage plane orientation of divisions in control and FGF-treated slices, measured live from 1.5 days up to 38 hours. Error bars indicate s.d. (control: 84 divisions, 12 slices, three experiments; FGF-treated: 86 divisions, seven slices, three experiments.) FGF treatment does not result in a significant change in cleavage plane orientation. One-way ANOVA comparison of cleavage plane orientation of cells in live control and FGF-treated tissue ($P=0.57$), alpha level set at 0.05. (D) Proportion of cells dividing non-apically ($>10 \mu\text{m}$ away from the apical surface) increases when tissue is treated with FGF. In fixed tissue $15 \pm 6\%$ of mitotic cells are found away from the apical surface (505 cells, in 12 sections from six embryos); in live control tissue, $20 \pm 4\%$ of divisions are non-apical (687 cells in 28 slices from 11 experiments). In FGF-treated tissue the proportion of non-apical divisions increases to $36 \pm 9\%$ (300 cells, in 10 slices from six experiments). An ANOVA test between live control and live FGF-treated tissue provides evidence that there is a 95% chance of a statistical difference between these two populations ($P=0.00004$). Error bars indicate s.d.

realigned along the basal surface. Together, these observations indicate that an early step in the birth of a neuron is a dramatic change in neuroepithelial cell polarity, as indicated by loss of apical contacts, followed by a reorganization of the microtubule cytoskeleton.

Modes and mechanisms regulating neuron production

We find that divisions taking place at the same time at the apical surface of the early neural tube can be symmetric divisions that generate two progenitors or two neurons, or asymmetric divisions

that produce a progenitor and a neuron. This appears to differ from cell behaviour in the mammalian cortex, where these modes of division are more clearly temporally or spatially separated (Cai et al., 2002; Haubensak et al., 2004; Miyata et al., 2004; Noctor et al., 2004). The time and position of neuron births from both symmetric and asymmetric divisions, which we observe in dorsal and intermediate regions of the early rostral spinal cord, suggest that these cells are reticular spinal interneurons (Sechrist and Bronner Fraser, 1991). Symmetric division is also a strategy used to generate some early neurons in the zebrafish hindbrain (Lyons et al., 2003), but this will quickly deplete the progenitor cell population and it is surprising that this mode of neuron production should take place so early in neurogenesis.

This is the first study in which mitotic spindle orientation and subsequent daughter cell fates have been monitored continuously in the vertebrate neural tube. Overall, perpendicular cleavage plane divisions generate daughter cells that adopt the same fates, but these can be either two neurons or two progenitors. As this occurs in the same tissue at the same time, this suggests that individual cells within this early neuroepithelium are not equivalent and that only some cells have neuron-generating (neurogenic) potential. This conclusion is supported by the peppered expression pattern of proneural bHLH transcription factors such as *Ng2* within the early spinal cord (Ma et al., 1999; Diez del Corral et al., 2003) (see Fig. S3 in the supplementary material). If this logic is applied to cell fate outcomes following non-perpendicular cleavage planes, it suggests that only those cells with neurogenic factors have the potential to generate a neuron and a progenitor, whereas non-neurogenic cells will continue to give rise to only progenitors, regardless of spindle orientation. Indeed, this is consistent with the daughter cell fates adopted following divisions with a parallel cleavage plane; most of these divisions give rise to two further progenitors. Overall, these data suggest that the mechanism of mitotic spindle orientation operates in the context of a heterogeneous cell population within the early spinal cord and that here assignment of neurogenic fate is not linked to division orientation.

Our data also reveal that NN division orientations are exclusively perpendicular and statistically distinct from those of both PN and PP divisions, whereas PN and PP division orientations are indistinguishable from each other. This suggests that mitotic spindle orientation is only crucial in neurogenic cells, where it distinguishes between stem cell and terminal modes of neuron production. This conclusion is consistent with data in the mammalian cortex showing that a slight deviation of the cleavage plane from 90° is sufficient to generate asymmetric fates in neurogenic cells (Kosodo et al., 2004), and with the increase in neurons born of terminal divisions following imposition of a perpendicular cleavage plane in this context (Sanada and Tsai, 2005). However, this contrasts with increased proliferation of some retinal cells following imposition of perpendicular cleavage plane divisions (Zigman et al., 2005), which indicates that here mitotic spindle orientation can regulate the switch to neuron production (see Harris, 2005).

Nevertheless, there is growing evidence that simply altering mitotic spindle orientation is not sufficient to elicit neuron production, as observed recently in the chick caudal neural tube prior to the normal onset of neuron production (Roszko et al., 2006) and, while our paper was under revision, in the *Drosophila* optic lobe (Egger et al., 2007). Furthermore, neurogenic determination prior to terminal mitosis has recently been reported in the zebrafish retina where it is mediated by *ath5* expression (Kay et al., 2005; Poggi et al., 2005). Determination of a neurogenic fate prior to mitoses that generate neurons in the chick neural tube is also suggested by *Ng2*-

positive cells, which rapidly incorporate BrdU (Murciano et al., 2002), and by the expression pattern of *Dyrk1a* (Hammerle et al., 2002).

Tis21, which distinguishes neurogenic divisions in mammalian neural tissue (Iacopetti et al., 1999; Kosodo et al., 2004), can drive cell cycle exit (Tirone, 2001) and it has been suggested that it functions to extend the G1 phase of the cell cycle, a characteristic of cells in the neuron-generating phase of cortical development (Calegari and Huttner, 2003; Takahashi et al., 1995) (reviewed by Gotz and Huttner, 2005). It also regulates expression of the neurogenic gene *Math1*, providing a link between neurogenic status and cell cycle control (Canzoniere et al., 2004). Based on studies in fixed tissue in the later hindbrain and early neural plate, cell cycle times in the early chick spinal cord have been estimated to be ~8 hours (Hammerle et al., 2002). Our calculations from BrdU labelling and direct measurements reveal a longer average cell-cycle time and a surprising heterogeneity in cell cycle times in the living neuroepithelium. Furthermore, as in the cortex, we show that neurogenic divisions are indeed longer than progenitor-generating divisions. The cell cycle preceding a symmetrical terminal division is predicted to be even longer than asymmetric neurogenic divisions (Calegari and Huttner, 2003). This may explain why to date we have not recorded the full cell cycle in a symmetric terminal division. This extension of cell cycle length in neurogenic divisions further helps to distinguish neurogenic from non-neurogenic progenitors.

Consistent with the link between neurogenic factors and cell cycle regulation (reviewed by Ohnuma and Harris, 2003), we further show that FGF-mediated inhibition of neuronal differentiation, which involves repression of neurogenic genes, also entails cell cycle acceleration, and a similar observation has been made in cortical progenitor cells in vitro (Lukaszewicz et al., 2002). FGF probably interferes with neurogenesis at multiple levels (Olivera-Martinez and Storey, 2007), and we also see an increase in non-apical divisions and breakdown of interkinetic nuclear migration in a subset of cells; a response difference that may reflect cell cycle phase on first exposure to FGF (Hitomi and Stacey, 1999). Finally, the lack of effect of FGF on the range of division orientations at the apical surface reinforces the observation that the mechanism of mitotic spindle position and the assignment of neurogenic cell fate are separable processes.

Development of a long-term live imaging assay in the spinal cord has allowed us to follow individual cells throughout neurogenesis. We have revealed great cell heterogeneity within this tissue, measured accurately mitotic spindle orientation, identified novel cell behaviour associated with neuronal differentiation and imaged continuously for long enough to ascertain cell fate outcomes following oriented divisions. Our observations confirm a link between cell cycle duration and neuron generation and support the important conclusion that although mitotic spindle orientation can regulate cell fate symmetry, it need not determine neurogenic cell fate. This new long-term, high-resolution imaging assay now opens the way to analysis of signalling dynamics on a cell-by-cell basis during neurogenesis in the spinal cord, and to detailed investigation of the links between the mechanics of mitosis and neuron production.

We are grateful to Ruth Diez del Corral for help establishing slice culture methods, Sam Swift for microscopy advice and support, Chris Allan for computing support, Janice Aitken for artwork of a stage 10 embryo, Jonathan Gordon and David Martin for statistical advice, and Jon Clarke, Ruth Diez del Corral, Domingos Henrique and an anonymous reviewer for critical reading of various versions of this manuscript. A.C.W. was supported by a

Wellcome Trust four-year PhD program studentship, J.R.S. is a Wellcome Trust Senior Research Fellow, and K.G.S. was an MRC Senior Non-Clinical Research Fellow when this work began and is currently funded by a grant from the MRC (G0600234).

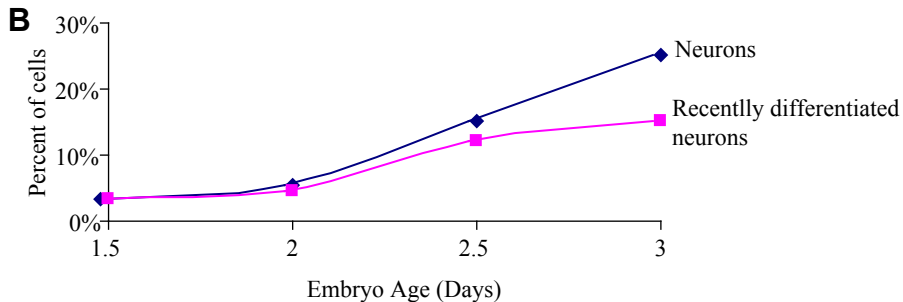
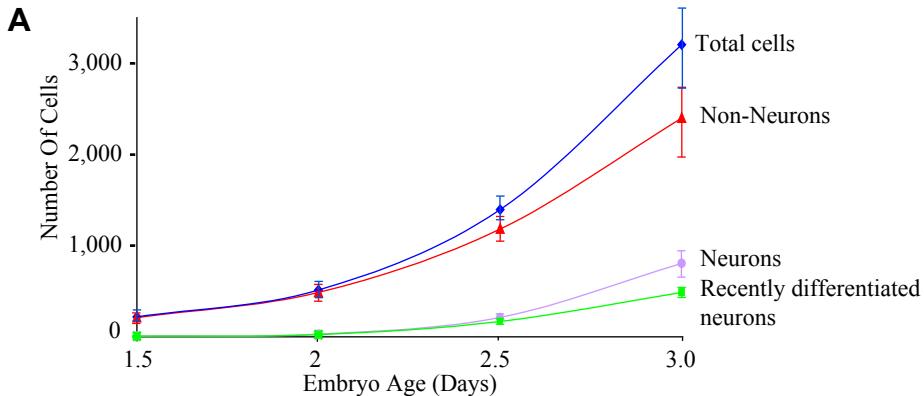
Supplementary material

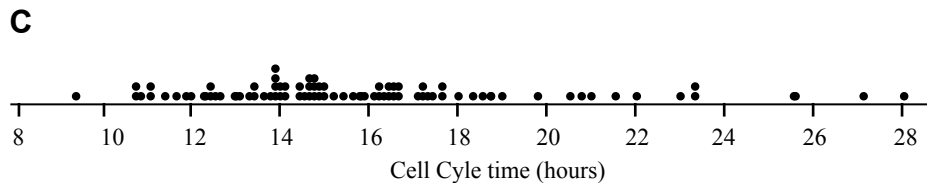
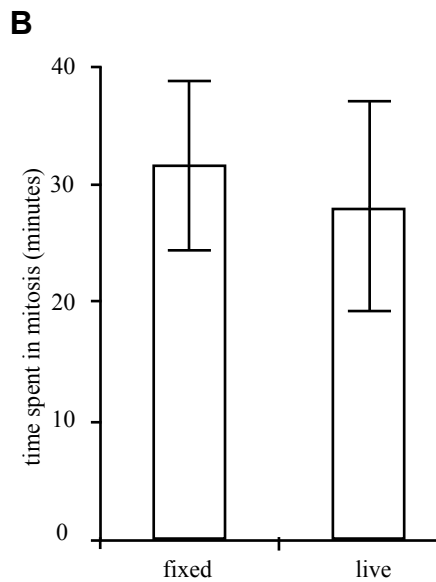
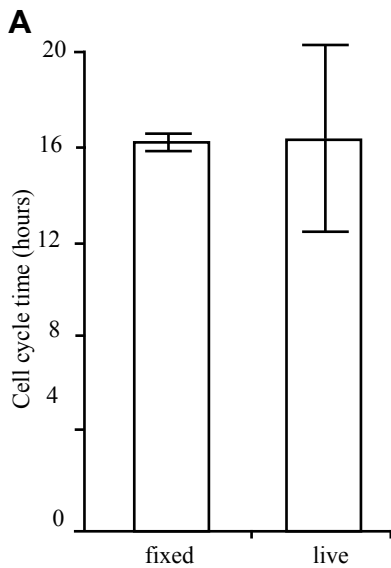
Supplementary material for this article is available at <http://dev.biologists.org/cgi/content/full/134/10/1943/DC1>

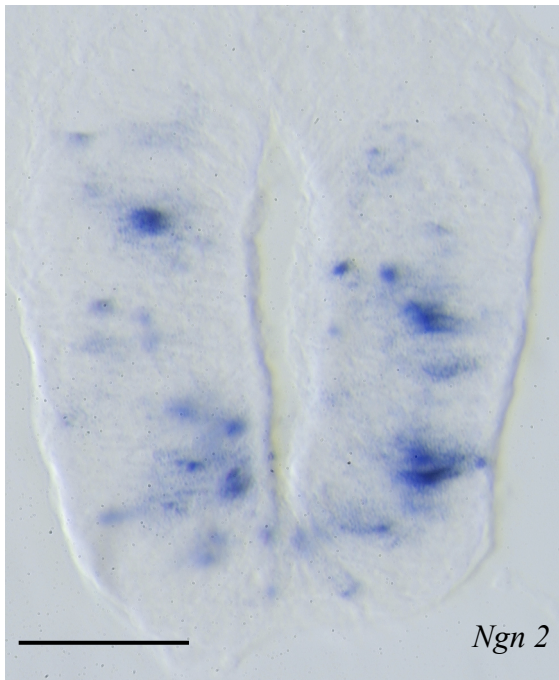
References

- Afonso, C. and Henrique, D. (2006). PAR3 acts as a molecular organizer to define the apical domain of chick neuroepithelial cells. *J. Cell Sci.* **119**, 4293-4304.
- Bertrand, N., Castro, D. S. and Guillemot, F. (2002). Proneural genes and the specification of neural cell types. *Nat. Rev. Neurosci.* **3**, 517-530.
- Betschinger, J. and Knoblich, J. A. (2004). Dare to be different: asymmetric cell division in *Drosophila*, *C. elegans* and vertebrates. *Curr. Biol.* **14**, R674-R685.
- Cai, L., Hayes, N. L., Takahashi, T., Caviness, V. S., Jr and Nowakowski, R. S. (2002). Size distribution of retrovirally marked lineages matches prediction from population measurements of cell cycle behavior. *J. Neurosci. Res.* **69**, 731-744.
- Calegari, F. and Huttner, W. B. (2003). An inhibition of cyclin-dependent kinases that lengthens, but does not arrest, neuroepithelial cell cycle induces premature neurogenesis. *J. Cell Sci.* **116**, 4947-4955.
- Calegari, F., Haubensak, W., Haffner, C. and Huttner, W. B. (2005). Selective lengthening of the cell cycle in the neurogenic subpopulation of neural progenitor cells during mouse brain development. *J. Neurosci.* **25**, 6533-6538.
- Canzoniere, D., Farioli-Vecchioli, S., Conti, F., Ciotti, M. T., Tata, A. M., Augusti-Tocco, G., Mattei, E., Lakshmana, M. K., Krizhanovsky, V., Reeves, S. A. et al. (2004). Dual control of neurogenesis by PC3 through cell cycle inhibition and induction of Math1. *J. Neurosci.* **24**, 3355-3369.
- Chenn, A. and McConnell, S. K. (1995). Cleavage orientation and the asymmetric inheritance of Notch1 immunoreactivity in mammalian neurogenesis. *Cell* **82**, 631-641.
- Das, T., Payer, B., Cayouette, M. and Harris, W. A. (2003). In vivo time-lapse imaging of cell divisions during neurogenesis in the developing zebrafish retina. *Neuron* **37**, 597-609.
- Diez del Corral, R., Brechtkreuz, D. N. and Storey, K. G. (2002). Onset of neuronal differentiation is regulated by paraxial mesoderm and requires attenuation of FGF signalling. *Development* **129**, 1681-1691.
- Diez del Corral, R., Olivera-Martinez, I., Goriely, A., Gale, E., Maden, M. and Storey, K. (2003). Opposing FGF and retinoid pathways control ventral neural pattern, neuronal differentiation, and segmentation during body axis extension. *Neuron* **40**, 65-79.
- Egger, B., Boone, J. Q., Stevens, N. R., Brand, A. H. and Doe, C. Q. (2007). Regulation of spindle orientation and neural stem cell fate in the *Drosophila* optic lobe. *Neural Dev.* **2**, 1.
- Frade, J. M. (2002). Interkinetic nuclear movement in the vertebrate neuroepithelium: encounters with an old acquaintance. *Prog. Brain Res.* **136**, 67-71.
- Glotzer, M. (2005). The molecular requirements for cytokinesis. *Science* **307**, 1735-1739.
- Gotz, M. and Huttner, W. B. (2005). The cell biology of neurogenesis. *Nat. Rev. Mol. Cell Biol.* **6**, 777-788.
- Gunhaga, L., Jessell, T. M. and Edlund, T. (2000). Sonic hedgehog signaling at gastrula stages specifies ventral telencephalic cells in the chick embryo. *Development* **127**, 3283-3293.
- Hamburger, H. and Hamilton, H. L. (1951). A series of normal stages in the development of the chick embryo. *J. Exp. Morphol.* **88**, 49-92.
- Hammerle, B., Vera-Samper, E., Speicher, S., Arenz, R., Martinez, S. and Tejedor, F. J. (2002). Mnb/Dyrk1A is transiently expressed and asymmetrically segregated in neural progenitor cells at the transition to neurogenic divisions. *Dev. Biol.* **246**, 259-273.
- Harris, W. A. (2005). Two of these or two of those? *Neuron* **48**, 521-522.
- Haubensak, W., Attardo, A., Denk, W. and Huttner, W. B. (2004). Neurons arise in the basal neuroepithelium of the early mammalian telencephalon: a major site of neurogenesis. *Proc. Natl. Acad. Sci. USA* **101**, 3196-3201.
- Haydar, T. F., Ang, E., Jr and Rakic, P. (2003). Mitotic spindle rotation and mode of cell division in the developing telencephalon. *Proc. Natl. Acad. Sci. USA* **100**, 2890-2895.
- Hitomi, M. and Stacey, D. W. (1999). Cyclin D1 production in cycling cells depends on ras in a cell-cycle-specific manner. *Curr. Biol.* **9**, 1075-1084.
- Iacopetti, P., Michelini, M., Stuckmann, I., Oback, B., Aaku-Saraste, E. and Huttner, W. B. (1999). Expression of the antiproliferative gene TIS21 at the onset of neurogenesis identifies single neuroepithelial cells that switch from proliferative to neuron-generating division. *Proc. Natl. Acad. Sci. USA* **96**, 4639-4644.
- Itasaki, N., Bel-Vialar, S. and Krumlauf, R. (1999). 'Shocking' developments in chick embryology: electroporation and in ovo gene expression. *Nat. Cell Biol.* **1**, E203-E207.
- Jessell, T. M. (2000). Neuronal specification in the spinal cord: inductive signals and transcriptional codes. *Nat. Rev. Genet.* **1**, 20-29.
- Kauffman, S. (1968). Lengthening of the generation time during embryonic differentiation of the mouse neural tube. *Exp. Cell Res.* **49**, 420-424.
- Kay, J. N., Link, B. A. and Baier, H. (2005). Staggered cell-intrinsic timing of ath5 expression underlies the wave of ganglion cell neurogenesis in the zebrafish retina. *Development* **132**, 2573-2585.
- Kosodo, Y., Roper, K., Haubensak, W., Marzesco, A. M., Corbeil, D. and Huttner, W. B. (2004). Asymmetric distribution of the apical plasma membrane during neurogenic divisions of mammalian neuroepithelial cells. *EMBO J.* **23**, 2314-2324.
- Lewis, J. (1996). Neurogenic genes and vertebrate neurogenesis. *Curr. Opin. Neurobiol.* **6**, 3-10.
- Lukaszewicz, A., Savatier, P., Cortay, V., Kennedy, H. and Dehay, C. (2002). Contrasting effects of basic fibroblast growth factor and neurotrophin 3 on cell cycle kinetics of mouse cortical stem cells. *J. Neurosci.* **22**, 6610-6622.
- Lyons, D. A., Guy, A. T. and Clarke, J. D. (2003). Monitoring neural progenitor fate through multiple rounds of division in an intact vertebrate brain. *Development* **130**, 3427-3436.
- Ma, Q., Fode, C., Guillemot, F. and Anderson, D. J. (1999). Neurogenin1 and neurogenin2 control two distinct waves of neurogenesis in developing dorsal root ganglia. *Genes Dev.* **13**, 1717-1728.
- Marusich, M. F., Furneaux, H. M., Henion, P. D. and Weston, J. A. (1994). Hu neuronal proteins are expressed in proliferating neurogenic cells. *J. Neurobiol.* **25**, 143-155.
- McNally, J. G., Karpova, T., Cooper, J. and Conchello, J. A. (1999). Three-dimensional imaging by deconvolution microscopy. *Methods* **19**, 373-385.
- Messier, P. E. and Auclair, C. (1974). Effect of cytochalasin B on interkinetic nuclear migration in the chick embryo. *Dev. Biol.* **36**, 218-223.
- Minaki, Y., Mizuhara, E., Morimoto, K., Nakatani, T., Sakamoto, Y., Inoue, Y., Satoh, K., Imai, T., Takai, Y. and Ono, Y. (2005). Migrating postmitotic neural precursor cells in the ventricular zone extend apical processes and form adherens junctions near the ventricle in the developing spinal cord. *Neurosci. Res.* **52**, 250-262.
- Miyata, T., Kawaguchi, A., Okano, H. and Ogawa, M. (2001). Asymmetric inheritance of radial glial fibers by cortical neurons. *Neuron* **31**, 727-741.
- Miyata, T., Kawaguchi, A., Saito, K., Kawano, M., Muto, T. and Ogawa, M. (2004). Asymmetric production of surface-dividing and non-surface-dividing cortical progenitor cells. *Development* **131**, 3133-3145.
- Murciano, A., Zamora, J., Lopez-Sanchez, J. and Frade, J. M. (2002). Interkinetic nuclear movement may provide spatial clues to the regulation of neurogenesis. *Mol. Cell. Neurosci.* **21**, 285-300.
- Nagele, R. G. and Lee, H. Y. (1979). Ultrastructural changes in cells associated with interkinetic nuclear migration in the developing chick neuroepithelium. *J. Exp. Zool.* **210**, 89-106.
- Noctor, S. C., Martinez-Cerdeno, V., Ivic, L. and Kriegstein, A. R. (2004). Cortical neurons arise in symmetric and asymmetric division zones and migrate through specific phases. *Nat. Neurosci.* **7**, 136-144.
- Ohnuma, S. and Harris, W. A. (2003). Neurogenesis and the cell cycle. *Neuron* **40**, 199-208.
- Olivera-Martinez, I. M. and Storey, K. G. (2007). Wnt signals provide a timing mechanism for the FGF-retinoid differentiation switch during vertebrate body axis extension. *Development* **134** (in press).
- Placzek, M. and Dale, K. (1999). Tissue recombinations in collagen gels. *Methods Mol. Biol.* **97**, 293-304.
- Poggi, L., Vitorino, M., Masai, I. and Harris, W. A. (2005). Influences on neural lineage and mode of division in the zebrafish retina in vivo. *J. Cell Biol.* **171**, 991-999.
- Price, S. R. and Briscoe, J. (2004). The generation and diversification of spinal motor neurons: signals and responses. *Mech. Dev.* **121**, 1103-1115.
- Roszko, I., Afonso, C., Henrique, D. and Mathis, L. (2006). Key role played by RhoA in the balance between planar and apico-basal cell divisions in the chick neuroepithelium. *Dev. Biol.* **298**, 212-224.
- Roztocil, T., Matter Sadzinski, L., Alliod, C., Ballivet, M. and Matter, J. M. (1997). NeuroM, a neural helix-loop-helix transcription factor, defines a new transition stage in neurogenesis. *Development* **124**, 3263-3272.
- Saito, K., Kawaguchi, A., Kashiwagi, S., Yasugi, S., Ogawa, M. and Miyata, T. (2003). Morphological asymmetry in dividing retinal progenitor cells. *Dev. Growth Differ.* **45**, 219-229.
- Sanada, K. and Tsai, L. H. (2005). G protein betagamma subunits and AGS3 control spindle orientation and asymmetric cell fate of cerebral cortical progenitors. *Cell* **122**, 119-131.
- Scardigli, R., Schuurmans, C., Gradwohl, G. and Guillemot, F. (2001). Crossregulation between Neurogenin2 and pathways specifying neuronal identity in the spinal cord. *Neuron* **31**, 203-217.
- Scardigli, R., Baumer, N., Gruss, P., Guillemot, F. and Le Roux, I. (2003). Direct and concentration-dependent regulation of the proneural gene Neurogenin2 by Pax6. *Development* **130**, 3269-3281.
- Sechrist, J. and Bronner Fraser, M. (1991). Birth and differentiation of reticular neurons in the chick hindbrain: ontogeny of the first neuronal population. *Neuron* **7**, 947-963.
- Skop, A. R., Liu, H., Yates, J., 3rd, Meyer, B. J. and Heald, R. (2004). Dissection

- of the mammalian midbody proteome reveals conserved cytokinesis mechanisms. *Science* **305**, 61-66.
- Storey, K. G.** (1989). Cell lineage and pattern formation in the earthworm embryo. *Development* **107**, 519-532.
- Swedlow, J. R., Sedat, J. W. and Agard, D. A.** (1997). *Deconvolution in Optical Microscopy*. New York: Academic Press.
- Takahashi, T., Nowakowski, R. S. and Caviness, V. S., Jr** (1995). The cell cycle of the pseudostratified ventricular epithelium of the embryonic murine cerebral wall. *J. Neurosci.* **15**, 6046-6057.
- Tirone, F.** (2001). The gene PC3(TIS21/BTG2), prototype member of the PC3/BTG/TOB family: regulator in control of cell growth, differentiation, and DNA repair? *J. Cell. Physiol.* **187**, 155-165.
- Wildner, H., Muller, T., Cho, S. H., Brohl, D., Cepko, C. L., Guillemot, F. and Birchmeier, C.** (2006). dILA neurons in the dorsal spinal cord are the product of terminal and non-terminal asymmetric progenitor cell divisions, and require Mash1 for their development. *Development* **133**, 2105-2113.
- Zigman, M., Cayouette, M., Charalambous, C., Schleiffer, A., Hoeller, O., Dunican, D., McCudden, C. R., Firnberg, N., Barres, B. A., Siderovski, D. P. et al.** (2005). Mammalian inscuteable regulates spindle orientation and cell fate in the developing retina. *Neuron* **48**, 539-545.







Ngn 2